Short Communication

Designing double-layered Si and Si/LATP nanocomposite anode for high-voltage aqueous lithium-ion batteries

Anjali Paravannoor[1] · Deepthi Panoth[1] · Pattathil Praveen[2]

Received: 3 May 2020 / Accepted: 25 September 2020 / Published online: 16 October 2020

Abstract
A novel anode design is demonstrated with Si nanostructures with double-layered protection for an aqueous rechargeable Li-ion Battery (ARLIB). Si nanoparticle-embedded LATP (lithium aluminum titanium phosphate; $Li_{1.3}Al_{0.3}Ti_{1.7}(PO_4)_3$), as well as LATP-PVDF polymer nanocomposites, is used as the protective layers. The unique anode structure is expected to be useful in overcoming the cathodic challenges and subsequent gas evolution reactions, thus widening the operating voltage of an ARLIB up to 3.5 V. The layered anodes exhibited discharge capacities of 2630 mAh g^{-1} at 0.1 C as half cells in 2 M Li_2SO_4 aqueous solution as the electrolyte. They are also coupled with $LiFePO_4$ cathode, and the full cells demonstrate a discharge capacity of 123 mAh g^{-1} with the calculated energy density values of 138 Wh kg^{-1} which is comparable with the conventional organic electrolyte-based LIBs. They can cycle 500 times with capacity retention of more than 75%. Hence, the conclusions from the present study project a promising anode design for ARLIBs, with high capacities and long cycling stabilities.

Keywords Li-ion battery · Aqueous electrolyte · Silicon anode · Layered anode · LATP

1 Introduction

Li-ion batteries are one of the most widely accepted technologies of choice when it comes to energy storage devices, especially for portable electronic applications [1–3]. Researches try to explore various possibilities of anode and cathode materials and electrolyte formulations to enhance the durability and energy efficiency of the system [4, 5]. However, the technology is often questioned for its safety as there are incidents involving high-profile explosions and these concerns hinder their applications in large-scale purposes, especially in electric vehicles and hybrid electric vehicles as they require large-format LIBs (> 30 Ah) [6]. One of the major challenges associated with the safe scaling up of conventional LIBs is the highly flammable organic electrolyte formulations that fuel the chemical combustion initiated by high energy electrode materials like Li metal which in turn would lead to thermal runaways [7, 8]. Since the energy density of the LIBs is not to be compromised, the obvious solution to address the associated disadvantages is to replace the highly inflammable organic electrolytes which project safety concerns also of their own [9].

One of the most suitable replacements for the carbonate ester-based conventional organic electrolytes is water which possesses additional advantages of its high values of dipole moment (1.8546 Debye), acceptor, and donor numbers (AN = 54.8, DN = 18) and dielectric constant (ε = 78 at 25 °C). The factor that hinders the use of aqueous electrolytes in LIBs is the low electrochemical stability

Electronic supplementary material The online version of this article (https://doi.org/10.1007/s42452-020-03592-3) contains supplementary material, which is available to authorized users.

✉ Anjali Paravannoor, anjali.nano@gmail.com | [1]School of Chemical Sciences, Swami Anandatheertha Campus, Kannur University, Edat P O, Payyannur, Kerala, India. [2]Suzlon Energy Limited, One Earth, Pune, Maharashtra 411028, India.

window of 1.23 V with its cathodic and anodic limits situated at 2.62 V and 3.85 V versus Li, respectively, and the redox potentials of most of the LIB anode materials are located far beyond these limits (e.g., Li metal, 0.0 V; graphite, 0.10 V; silicon, 0.30 V) [10, 11].

Even with the promising results of "water-in-salt" electrolytes (WiSE) with high salt concentration, which kinetically protect the electrode surfaces from operating above the limits, the energy density values offered by these designs are still far below as compared to the state-of-the-art LIB designs [12, 13]. This difference could be attributed to the cathodic limitation since the most energy-dense anode materials like Li, graphite, and alloy anodes are all located below the 1.7 V limit. To overcome these limitations, the anode requires a protective coating which would hinder the accumulation and subsequent hydrogen evolution happening before the solid electrolyte interphase (SEI) layer formation [14]. Even though there are very few studies on this concept wherein the protected Li metal and graphite anodes are used as anodes for Li secondary batteries, alloy anodes like Si and Ge are seldom explored while they are the class of anode materials with the highest theoretical capacity as well as moderate anodic voltage reported in the literature [15–17].

However, owing to the low theoretical capacity of graphite and the possibility of breaking the protective coating which could lead to a vigorous reaction between Li and water, alloy anodes could be potential candidates to be approached in this concept. With these remarks, the present study reports a silicon-based anode material with a unique double-layer assembly with one layer composed of a LATP/Si plum pudding-like structure and another layer of pristine Si. In situ synthesis of the electrode material along with a Li superionic conductor like LATP is followed as it would be beneficial in decreasing the interfacial resistance as reported in the previous literature [18].

2 Results and discussion

The layered anode structure was synthesized using Si, Si-LATP plum pudding-like structure, and another LATP layer blended with hydrophobic PVDF polymer. A detailed description of the experimental methods for the synthesis of active materials, fabrication of electrodes and cells as well as the morphological and electrochemical characterizations are included in the Supplementary Information (SI-I).

2.1 Structural and morphological characterizations

Figure 1a shows the XRD spectra of Si-LATP samples. The presence of phase pure Si was evident from the spectra

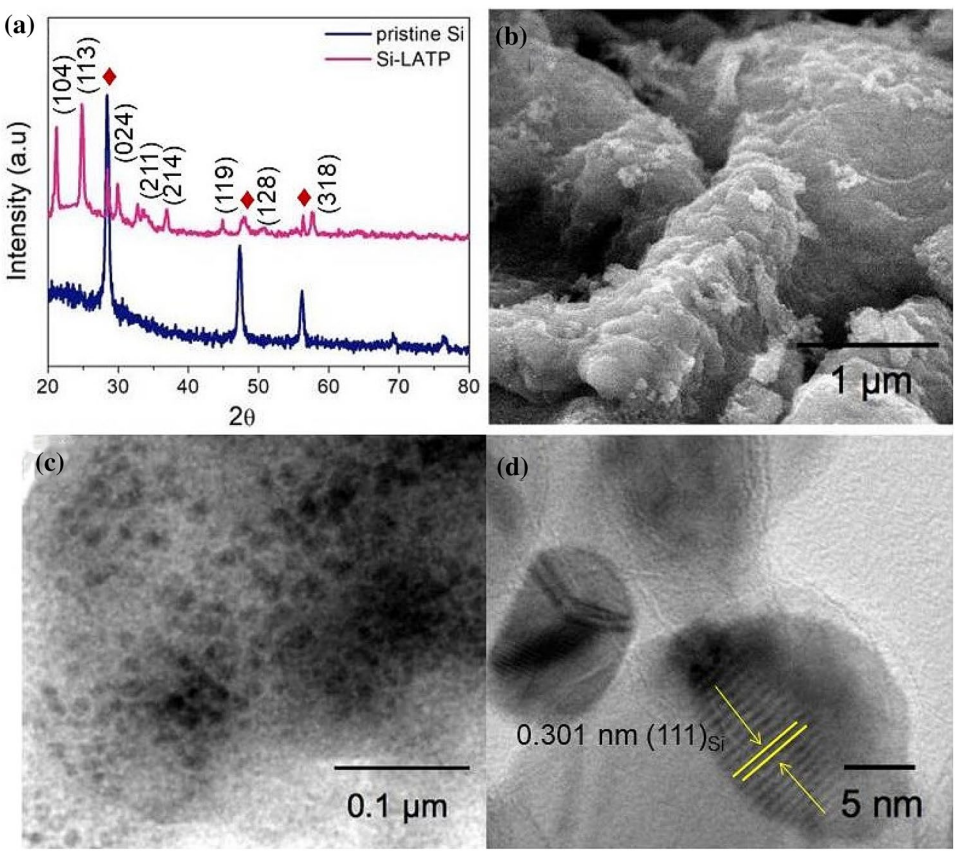

Fig. 1 **a** XRD of Si-LATP and pristine Si samples **b** SEM **c** TEM and **d** HR-TEM micrographs of Si-LATP samples

(JCPDS No. 27-1402). It was also found that the LATP-Si sample shows the presence of well-crystallized peaks of NASICON structured LATP (hexagonal setting of the rhombohedral space group (S.G. R-3c), (JCPDS No.40-0095) [19–21].

Figure 1b shows the Scanning electron microscopy (SEM) images illustrating the surface morphology of LATP-Si composite film demonstrating a homogeneous morphology. Figure 1 c shows the low-magnification transmission electron microscopy (TEM) images of Si-LATP structure denoting the uniform dispersion of Si nanoparticles in the LATP matrix. In order to further analyze the structural details, high-resolution TEM (HRTEM) images are taken (Fig. 1d) and it was found that the Si nanoparticles have a spherical morphology with a diameter of 20–40 nm. Figure 2e shows the lattice spacing's at the interface the Si nanoparticles were found to be crystalline with the d spacing of ~0.301 nm by the (111) planes of crystalline Si. The morphological characterizations of pristine Si as well as pristine LATP have been included in the supplementary information (SI-II). The composition of the LATP-Si samples was also evaluated using inductively coupled plasma (ICP) elementary analyses to confirm the final composition of the samples. The results obtained are given in the Supplementary Information revealing an elemental composition that corresponds to the theoretical stoichiometry of $Li_{1+x}Al_xTi_{2-x}(PO_4)_3$ with x = 0.3 as assumed (SI-III).

2.2 Electrochemical characterizations

Figure 2 illustrates the schematic illustration of the silicon-based anode with the double-layer structure. The initial layer consists of pristine Si nanoparticle, whereas the second layer consists of a plum pudding-like structure with silicon nanostructures embedded in a LATP matrix. The double-layer electrode is coated with a PVDF-LATP composite electrolyte layer which can also act as a separator. The coated silicon anode is expected to be very stable in an aqueous electrolyte background.

Figure 3a, b shows the CV curve of the double-layer Si-based anode and $LiFePO_4$ obtained in a 0.5 molar Li_2SO_4 aqueous solution. Platinum (Pt) mesh is used as the counter electrode and saturated calomel electrode (SCE) as the reference electrode. To better understand the real scenario, the potential has been converted to a Li/Li + reference. Figure 3a shows the CV curves of the layered anode at 1st, 2nd, and 5th cycles. The peak at around 0.3 V that appears from the second cycle could be assigned to the Li alloying process. The peak is not present in the initial cycle which could be attributed to the required activation of silicon. CV curves showing a comparison with pristine LATP in aqueous solution and pristine Si in 1 M $LiPF_6$ in EC/DEC have been included in the Supplementary Information (SI-IV) for the superior understanding of the performance of the layered structure. It is well evidenced that the Li alloying/dealloying process does occur in the Si anode with

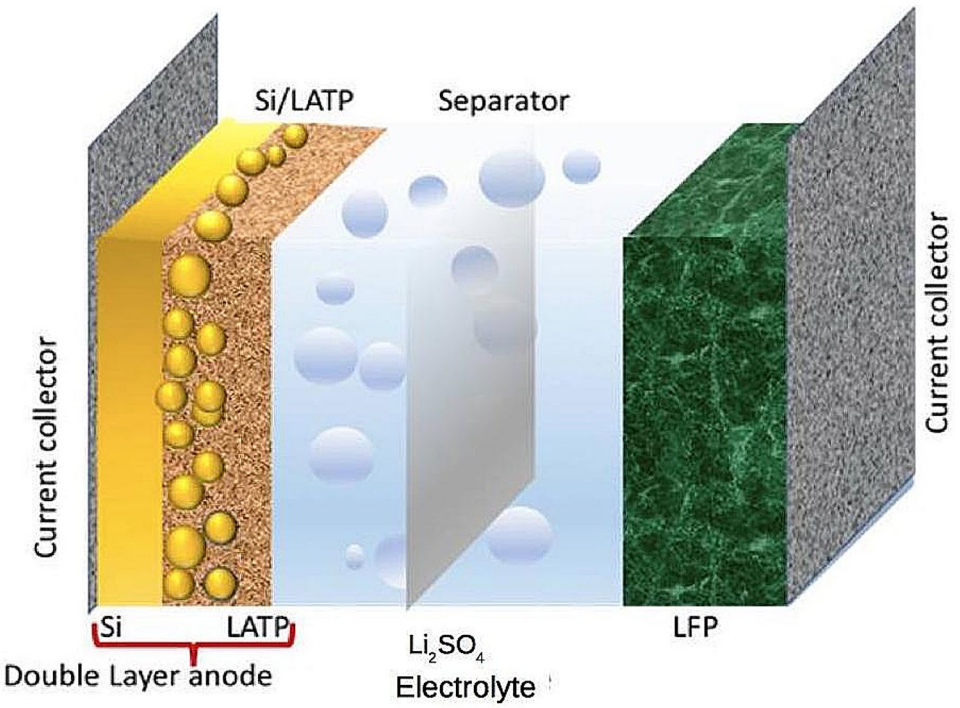

Fig. 2 Schematic illustration of the cell design

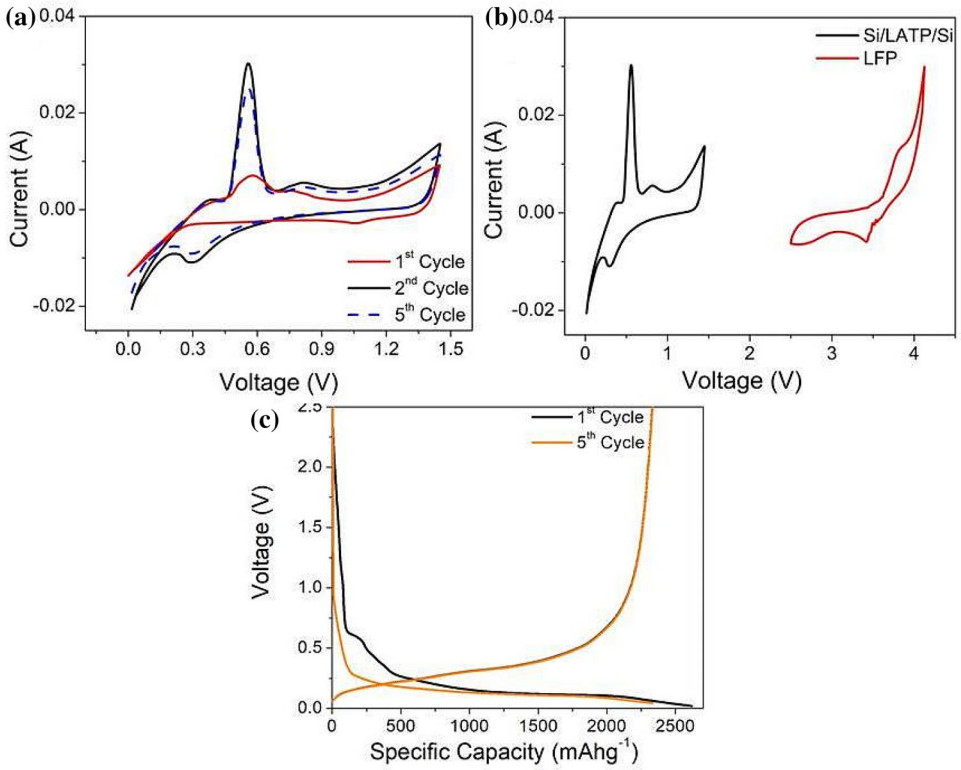

Fig. 3 **a** CV curves of the layered anode structure at 1st, 2nd, and 5th cycles **b** CV curves of cathode and anode (vs. Li/Li+) and **c** charge–discharge cycles of the anode at 1st and 5th Cycles

the Li+ ions passing through the polymer-LATP membrane between Si and the aqueous electrolyte. The small peak appearing in the cathodic scan at about 1 V could be attributed to the initial formation of the SEI layer. The LATP, while acting like a protective layer, could also contribute towards the anode capacity as evidenced by the CV curves. It is well versed in the literature that LATP does take part in the redox reaction (Ti^{4+}/Ti^{3+}) while the $Li_{1.3}Al_{0.3}Ti_{1.7}(PO_3)_4$ is converted to $Li_3Al_{0.3}Ti_{1.7}(PO_3)_4$ [22]. The significant factor is that the reduced form of LATP maintains the NASICON structure and Li superionic conductivity and has also got a better diffusion and higher ion conductivity of Lithium [23].

However, it disappears in consecutive cycles. Figure 3b displays the graph showing CV curves performed on Si anode together with a $LiFePO_4$ cathode material with a delithiation potential centered around at reaction occurred at 3.8 V. Now, it can be assumed that coupling of the double-layer Si anode with the $LiFePO_4$ cathode would form an aqueous LIB of > 3 V. Since the potential of the Si anode lies far below the potential for hydrogen evolution reaction, it is expected that hydrogen evolution happens in an aqueous electrolyte-based system.

However, it is prevented by the unique design of the anode wherein the Si nanoparticles are protected by the LATP-polymer matrix. Since only Li^+ ions and not water or protons could enter inside the coating, due to the unique properties of LATP together with the presence of the hydrophobic polymer, hydrogen production is prevented [22–25]. Moreover, the Li^+ ions outside the coating are in a very stable position with a higher potential without taking part in the gas evolution process. In addition to the protective properties of LATP in the system, the unique layered anode design aids in reducing the interfacial layer which would be higher in the absence of the composite layer. This is validated by the ex situ SEM images of the Si-LATP-Si interface at 1st and 5th cycles with a continuous uniform interface exhibited in the presence of Si-LATP intermediate layer, whereas in the absence of such an intermediate layer, a cracked interface is visible which in turn would increase the resistance and affect the rate performance (Supplementary Information SI-V). It is attributed that the alloy formation during the initial cycles from both the layers prevents any cracks or separation between the layers. At the same time, since the LATP is only conducting Li^+ ions, the extend of SEI layer formation is minimal which would prevent cracking of the Si active material, hence enhancing the stability. To further analyze the electrochemical characteristics of the anode, especially to analyze the efficiency and stability of the novel design, galvanostatic tests were conducted, where the layered anode was lithiated and delithiated at constant current (Fig. 3c). The discharge profiles of the electrode shows a clear indication of the Li alloying process delivering a discharge capacity of 1494 mAh g^{-1}. The Coulombic efficiency (CE%) of the electrodes at the 1st and 5th cycle was

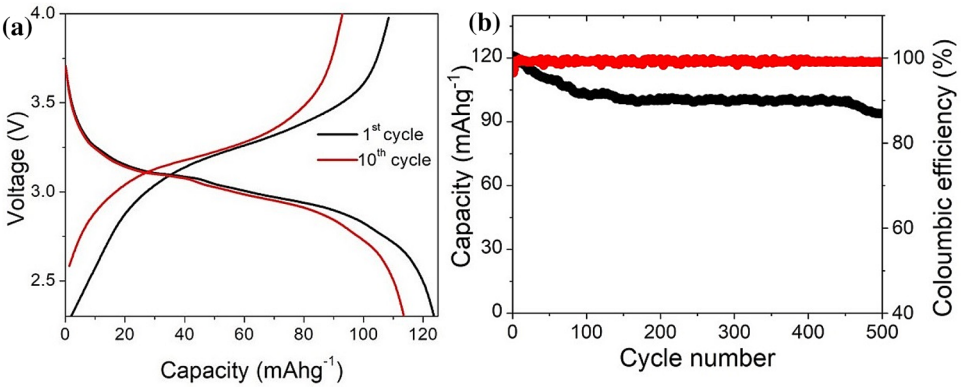

Fig. 4 **a** Charge discharge cycles at 1st and 10th cycles and **b** curves showing the cyclic stability and Coulombic efficiency of the full cells

calculated to be 88 and 99.6%, respectively. This could be attributed to the formation of an interface at the Si/LATP double-layer region [17]. The tiny plateau at around 0.6 V could be correlated with the additional reactions happening below 0.8 V contributed by the LATP component. The $[PO_4]$ tetrahedra in LATP act as an electron donor/acceptor during the intercalation and deintercalation of Li ions within the LATP crystal structure [22]. Since this feature is absent in the CV curves, the CV studies were also done at a lower scan rate of 0.1 mV s^{-1} where the peaks at around 0.58 V appeared (SI-IV (b)). Moreover, to further confirm the stability of the anode against H_2 evolution reactions, Linear Sweep Voltammetry studies were also carried out at a scan rate of 0.5 mV s^{-1} with Pt and SCE electrodes as the counter and reference electrodes, respectively.

As evidenced by the electrochemical analyses, the newly designed Si anodes show very promising performance in aqueous electrolyte systems, and to analyze the real scenario, they were coupled with a $LiFePO_4$ cathode material. Figure 4 shows the charge–discharge curves as well as the cyclic stability of the cells at room temperature. The full aqueous LIBs operate reversibly at or above 3.0 V plateaus for a continuous 500 cycles, and the capacities delivered were 124 mAh g^{-1}, a value comparable with similar systems in organic electrolytes. The CV characteristics of the full cell have also been analyzed and are given in the Supplementary Information (SI-IV (d)).

The energy density was calculated to be 138 Wh kg^{-1}, again making a reasonable value considering the fact that the representative Li-ion batteries based on organic electrolytes for electric vehicles are specified to be of 120 Wh kg^{-1}(C/ Organic Electrolyte/ $LiMn_2O_4$) [26]. The cyclic stability was found to be as high as 75% at the end of 500 cycles.

3 Conclusions

In conclusion, a highly safe aqueous rechargeable Li-ion battery is fabricated with an electrochemical stability window as high as 3.5 V. A layered anode design is adopted which would enable multiple advantages such as to overcome the cathodic limitation and the hydrogen evolution, decrease the interfacial resistance, and act as an artificial SEI layer. Three electrode studies exhibit discharge profiles that are indicative of the Li alloying process delivering a discharge capacity of 1494 mAh g^{-1}. The full cell in combination with $LiFePO_4$ exhibits a reasonable energy density of 138 Wh/Kg that is even comparable with an organic electrolyte-based lithium batteries.

Acknowledgments Department of Science and Technology (DST), Government of India, is gratefully acknowledged for their financial support to Dr. Anjali Paravannoor under the INSPIRE Faculty Scheme (Grant No: DST/INSPIRE/04/2015/001803).

Compliance with ethical standards

Conflict of interest On behalf of all authors, the corresponding author states that there is no conflict of interest.

References

1. Whittingham MS (2004) Li batteries and cathode materials. Chem Rev 104:4271–4302
2. Etacheri V, Marom R, Elazari R, Salitra GD, Aurbach (2011) Challenges in the development of advanced Li-ion batteries: a review. Energy Environ Sci 4:3243–3262
3. Evarts EC (2015) Lithium batteries: To the limits of lithium. Nature 526:S93–S95
4. Pavithra NS, Patil SB, Kumar SK, Alharthi FA, Nagaraju G (2019) Facile synthesis of nanocrystalline β-SnWO 4: as a photocatalyst, biosensor, and anode for Li-ion battery. SN ApplSci 1:1123
5. Xing A, Zhang J, Wang R, Wang J, Liu X (2019) Fly ashes as a sustainable source for nanostructured Si anodes in lithium-ion batteries. SN ApplSci 2:181

6. Wang K, Huang J (2019) Natural cellulose derived nanofibrous Ag-nanoparticle/ SnO_2/carbon ternary composite as an anodic material for lithium-ion batteries. J Phys Chem Solids 126:155–163
7. Wu H, Chan G, Choi JW, Ryu I, Yao Y, McDowell MT, Lee SW, Jackson A, Yang Y, Hu L, Cui Y (2012) Stable cycling of double-walled silicon nanotube battery anodes through solid-electrolyte interphase control. Nat Nanotechnol 7:310–315
8. Wang Q, Ping P, Zhao X, Chu G, Sun J, Chen C (2012) Thermal runaway caused fire and explosion of lithium ion battery. J Power Sources 208:210–224
9. Bandhauer TM, Garimella S, Fuller TF (2011) A critical review of thermal issues in lithium-ion batteries. J Electrochem Soc 158(3):R1–R25
10. Chawla N, Bharti N, Singh S (2019) Recent advances in non-flammable electrolytes for safer lithium-ion batteries. Batteries 5(1):19
11. Zhang WJ (2011) A review of the electrochemical performance of alloy anodes for lithium-ion batteries. J Power Sources 196:13–24
12. Jian G, Shi SQ, Li H (2016) Brief overview of electrochemical potential in lithium ion batteries. Chin Phys B 25:018210
13. Suo L, Han F, Fan X, Liu H, Xu K, Wang C (2016) "Water-in-Salt" electrolytes enable green and safe Li-ion batteries for large scale electric energy storage applications. J Mater Chem A 4:6639–6644
14. Lukatskaya MR, Feldblyum MJI, Mackanic DG, Lissel F, Michels DL, Cui Y, Bao Z (2018) Concentrated mixed cation acetate "water-in-salt" solutions as green and low-cost high voltage electrolytes for aqueous batteries. Energy Environ Sci 11:2876–2883
15. Wang H, Tang W, Ni L, Ma W, Chen G, Zhang N, Liu X, Ma R (2020) Synthesis of silicon nanosheets from kaolinite as a high-performance anode material for lithium-ion batteries. J Phys Chem Solids 137:109227
16. Azadeh M, Zamani C, Ataie A, Morante JR, Setoudeh N (2019) Role of milling parameters on the mechano-chemically synthesized mesoporous nanosilicon properties for Li-ion batteries anode. J Phys Chem Solids 20:109318
17. Wang X, Hou Y, Zhu Y, Wu Y, Holze R (2013) An aqueous rechargeable lithium battery using coated Li metal as anode. Sci Rep 3:401
18. Yang C, Chen J, Qing T, Fan X, Sun W, von Cresce A, Ding MS, Borodin O, Vatamanu J, Chroeder MA, Eidson N (2017) 4.0 V aqueous Li-ion batteries. Joule 1:122–132
19. Deiner LJ, Howell TG, Koenig GM, Rottmayer MA (2019) Interfacial reaction during co-sintering of lithium manganese nickel oxide and lithium aluminum germanium phosphate. Int J Appl Ceram Technol 16:1659–1667
20. Kimpa MI, Mayzan MZH, Esa F, Yabagi JA, Nmaya MM, Agam MA (2017) Sol–Gel synthesis and electrical characterization of $Li_{1+x}Al_xTi_{2-x}(PO_4)_3$ solid electrolytes. J SciTechnol 9:106–112
21. Ma F, Zhao E, Zhu S, Yan W, Sun D, Jin Y, Nan C (2016) Preparation and evaluation of high lithium ion conductivity $Li_{1.3}Al_{0.3}Ti_{1.7}(PO_4)_3$ solid electrolyte obtained using a new solution method. Solid state Ion 295:7–12
22. Augustin CA, Panoth D, Paravannoor A (2019) High Performance Li-ion battery Anodes based on Si Nano core in an LATP Matrix with better electrolyte compatibility and temperature resistance. ChemistrySelect 4:7090–7095
23. Bhanja P, Senthil C, Patra AK, Sasidharan M, Bhaumik A (2017) Microporous Mesoporous Mater 240:57–64
24. Chen L, Guo Z, Xia Y, Wang Y (2013) High voltage aqueous rechargeble battery approaching 3V using an acidic-alkaline dual electrolyte. ChemComm 49:2204–2207
25. Wang YG, Zhou HS (2010) A lithium-air battery with a potential to continuously reduce O_2 from air for delivering energy. J Power Sources 195:358–361
26. Wu YP, Yuan XY, Dong C, Duan JY (2012) Lithium ion batteries: applications and Practice, 2nd edn. Chemical Industry Press, Beijing